

RESEARCH LETTER

10.1002/2017GL076950

Key Points:

- We have performed the first comprehensive whole-atmosphere climate change simulations, including the thermosphere and ionosphere
- Results for solar minimum conditions indicate slow warming in the troposphere, changing to rapid cooling in the upper atmosphere
- In the mesopause region, systematic change was very small but exhibited considerable interannual variability

Correspondence to:

S. C. Solomon,
stans@ucar.edu

Citation:

Solomon, S. C., Liu, H.-L., Marsh, D. R., McInerney, J. M., Qian, L., & Vitt, F. M. (2018). Whole atmosphere simulation of anthropogenic climate change. *Geophysical Research Letters*, 45. <https://doi.org/10.1002/2017GL076950>

Received 27 DEC 2017

Accepted 19 JAN 2018

Accepted article online 24 JAN 2018

Whole Atmosphere Simulation of Anthropogenic Climate Change

Stanley C. Solomon¹ , Han-Li Liu¹ , Daniel R. Marsh¹ , Joseph M. McInerney¹ , Liying Qian¹ , and Francis M. Vitt¹ 
¹High Altitude Observatory, National Center for Atmospheric Research, Boulder, CO, USA

Abstract We simulated anthropogenic global change through the entire atmosphere, including the thermosphere and ionosphere, using the Whole Atmosphere Community Climate Model-eXtended. The basic result was that even as the lower atmosphere gradually warms, the upper atmosphere rapidly cools. The simulations employed constant low solar activity conditions, to remove the effects of variable solar and geomagnetic activity. Global mean annual mean temperature increased at a rate of +0.2 K/decade at the surface and +0.4 K/decade in the upper troposphere but decreased by about −1 K/decade in the stratosphere-mesosphere and −2.8 K/decade in the thermosphere. Near the mesopause, temperature decreases were small compared to the interannual variation, so trends in that region are uncertain. Results were similar to previous modeling confined to specific atmospheric levels and compared favorably with available measurements. These simulations demonstrate the ability of a single comprehensive numerical model to characterize global change throughout the atmosphere.

Plain Language Summary We performed the first whole-atmosphere simulations of global change that include the lower atmosphere (0–15 km), middle atmosphere (15–90 km), and thermosphere-ionosphere (90–500 km). All significant known changes caused by human activity were included in a new version of the Whole Atmosphere Community Climate Model-eXtended. The basic result is that even as the lower atmosphere gradually warms, the upper atmosphere rapidly cools. Simulations were conducted using constant low solar activity conditions, in order to remove the effects of the solar cycle on the upper atmosphere. Global mean annual average temperature increased at a rate of +0.2 K/decade at the surface and +0.4 K/decade about 10 km above the surface but decreased throughout the upper atmosphere, from about 20 km to 500 km, reaching −2.8 K/decade above 200 km. Near 90 km, very small temperature decreases were calculated, but the year-to-year variation was large, so temperature trends in that altitude region are uncertain. Results were similar to those obtained from previous work using numerical models that were confined to specific atmospheric levels and compare favorably with available measurements. These simulations demonstrate the ability of a single comprehensive numerical model to characterize global change throughout the atmosphere.

1. Introduction

The increase of atmospheric trace gases that absorb and radiate in the infrared, primarily due to anthropogenic sources, has caused the Earth's surface and troposphere to increase in temperature, especially since the mid-1900s. Above the tropopause, however, the atmosphere has cooled, because as atmospheric density decreases with altitude, the infrared bands that enable these trace gases to absorb and emit radiation become more optically thin, and radiative cooling begins to dominate over absorption and warming. This phenomenon has been recognized since the paper by Roble and Dickinson (1989) that predicted cooling of the mesosphere and thermosphere and earlier work that established stratospheric effects (Brasseur & Hitchman, 1988; Fels et al., 1980; Labitzke et al., 1986) and mesosphere-thermosphere cooling (Dickinson, 1984). The primary anthropogenic trace gas driving these changes is carbon dioxide (CO₂), but methane (CH₄) and chlorofluorocarbon (CFCs) species that cause depletion of stratospheric ozone (O₃) also play a role. Extensive observational work has since established the approximate rate of global temperature increase in the troposphere (e.g., Hansen et al., 2010) and estimated the temperature decreases in the upper atmosphere, as reviewed by Beig et al. (2003), Laštovička (2017), Laštovička et al. (2006, 2012), Qian et al. (2011), and references therein. The rate of upper atmosphere cooling varies considerably with altitude, and is difficult to measure in some ranges, but the evidence is most conclusive in the thermosphere, where

decreases in neutral density and temperature inferred from observations of the effect of atmospheric drag on satellite orbits have shown the most dramatic climate change of any altitude region (Emmert et al., 2004, 2008; Keating et al., 2000; Marcos et al., 2005; Saunders et al., 2011), confirming the predictions by Roble and Dickinson (1989). Subsequent modeling work in the mesosphere-thermosphere (e.g., Akmaev, 2012; Akmaev & Fomichev, 2000; Qian et al., 2013, 2006, 2014; Rishbeth & Roble, 1992; Solomon et al., 2015) and in the stratosphere-mesosphere (e.g., Akmaev, Fomichev, & Zhu, 2006; Fomichev et al., 2007; Garcia et al., 2007; Lübken et al., 2013) extended the analysis and clarified the mechanisms. In these model simulations, CO₂ is the dominant driver of temperature change, but CH₄, O₃, and possibly water vapor (H₂O) play significant roles in the stratosphere and mesosphere.

Together with the extensive efforts to model and measure climate change in the oceans, land masses, and troposphere, these piecewise model results present a nearly complete description of anthropogenic climate change throughout the atmosphere. However, a comprehensive single-model simulation that extends into the thermosphere and ionosphere has not previously been attempted. Our objective in this study was to perform an integrated simulation of all atmospheric regions that included a complete treatment of dynamics, chemistry, and radiative transfer. We used the National Center for Atmospheric Research (NCAR) Whole Atmosphere Community Climate Model-eXtended (WACCM-X) to examine the effects of anthropogenic global temperature change due to all known greenhouse gas emissions, including CO₂, CH₄, and CFCs. The studies were conducted for solar minimum conditions over a ~30 year time period. We compared these model simulations to the available data on secular trends as a function of altitude and to previous work that addressed various segments of the atmosphere.

2. Model Description

WACCM-X is a global general circulation model that calculates 3-D temperature, density, wind, composition, ionospheric, and electric potential fields from the surface to the exobase. It is a configuration of the NCAR Community Earth System Model (CESM) (Hurrell et al., 2013) and thus is uniquely capable of coupling to dynamic or specified ocean, land, and ice models. WACCM-X is based on the Community Atmosphere Model (CAM) component of CESM and incorporates the physics and chemistry of “regular” WACCM, which has an upper boundary of ~130 km but does not include an interactive ionosphere. The thermosphere and ionosphere components of WACCM-X add major and minor neutral species composition, electron, and ion density and composition, and electron and ion temperature, using methods originating with model predecessors (Richmond et al., 1992; Roble et al., 1988; Roble & Ridley, 1994). The model assumes hydrostatic equilibrium and uses a log-pressure coordinate system, with the pressure levels extending from 0 to ~600 km in altitude; the height of the upper boundary is dependent on solar activity. The simulations employed here use 1.9° × 2.5° horizontal resolution and 0.25 scale height vertical resolution above 1 hPa. Solar ultraviolet irradiance is parameterized using proxy models or supplied by measurements (Solomon & Qian, 2005). Auroral particle precipitation and an imposed magnetospheric electric field are estimated using the geomagnetic *K_p* index. Gravity wave effects are parameterized based on the linear saturation theory of Lindzen (1981). In the mesosphere and lower thermosphere region, a radiative transfer algorithm for CO₂ that was developed by Fomichev et al. (1998) is employed. For the basic formulation of WACCM and WACCM-X, see Marsh et al. (2007) and Liu et al. (2010). Recent developments, resulting in the impending release of WACCM-X v. 2.0 as part of CESM v. 2.0, include an interactive low-latitude electric field and ionospheric dynamical transport, which are described in Liu et al. (2018). However, WACCM-X is currently based on CAM4 and WACCM4 physics and chemistry (Marsh et al., 2013; Neale et al., 2013), as released in CESM v. 1.0, and thus lags the new version of CESM by a generation. The simulations shown here were conducted with a prerelease trunk version of WACCM-X v. 2.0, internally designated 5.4.99. The model can be used in either a free-running climate mode or with imposed meteorology analysis fields in the troposphere-stratosphere; see Marsh et al. (2013) for further discussion of chemistry, radiative transfer, and other forcings such as volcanic aerosols.

3. Climate Change Simulations

Simulations were conducted for perpetual solar minimum conditions, in order to eliminate the effects of solar irradiance and geomagnetic activity variation, which can be very significant above the mesopause. The approach employed was to conduct a 5 year simulation for the years 1972–1976 and compare it to a

Table 1
Model Inputs and Key Results

Inputs	1972–1976	2001–2005	Change per decade
$\langle \text{CO}_2 \rangle$ at surface	330 ppmv	375 ppmv	+16 ppmv
$\langle \text{CH}_4 \rangle$ at surface	1.44 ppmv	1.74 ppmv	+0.1 ppmv
$\langle \text{CFC11} + \text{CFC12} \rangle$ at surface	0.29 ppbv	0.79 ppbv	+0.2 ppbv
$F_{10.7}$ index	70	70	0
K_p index	0.3	0.3	0
Results	1972–1976	2001–2005	Change per decade
$\langle T \rangle$ at surface	287.8 K	288.4 K	+0.2 K
$\langle T \rangle$ at 10 km (266 hPa)	225.8 K	226.9 K	+0.4 K
$\langle T \rangle$ at tropopause	204.2 K	204.5 K	+0.1 K
$\langle T \rangle$ at stratopause	262.9 K	259.6 K	−1.1 K
$\langle T \rangle$ at mesopause	193.1 K	191.0 K	−0.7 K
$\langle T \rangle$ at 400 km	697.9 K	689.9 K	−2.8 K
$\langle \rho \rangle$ at 400 km (mass density)	0.584 ng m^{-3}	0.518 ng m^{-3}	−3.9%
$\langle NmF_2 \rangle$ (peak ion density)	$1.78 \times 10^5 \text{ cm}^{-3}$	$1.71 \times 10^5 \text{ cm}^{-3}$	−1.2%
$\langle h_m F_2 \rangle$ (height of peak)	261.5 km	257.8 km	−1.3 km
$\langle T_i \rangle$ at $h_m F_2$ (ion temperature)	712.8 K	704.9 K	−2.7 K
Other results for $\langle \rho \rangle$ at 400 km: observations	Comments	Change per decade	
Keating et al. (2000)	Low solar activity only	−5.0 ± 1.4%	
Marcos et al. (2005)	Average solar activity	−1.7 to −2.4%	
Emmert et al. (2008)	For low solar activity	−5.5 ± 1.4%	
Saunders et al. (2011)	For low-to-moderate solar activity	−7.2%	
Emmert (2015)	For all solar activity levels	−3.0 ± 1.0%	
Other results for $\langle \rho \rangle$ at 400 km: models	Comments	Change per decade	
Roble and Dickinson (1989)	Low-to-moderate solar activity ^a	~ −3%	
Rishbeth and Roble (1992)	Low-to-moderate solar activity ^a	~ −2%	
Qian et al. (2006)	For low solar activity	−2.5%	
Akmaev & Fomichev (2000), Akmaev et al. (2006)	At ~200 km altitude	−3 to −5%	
Solomon et al. (2015)	For low solar activity	−4.9%	
This work	Low solar activity only	−3.9%	

^aEstimated from doubling scenario.

5 year simulation for the years 2001–2005. The purpose of the 5 year interval was to serve as a small ensemble, in order to reduce the effect of interannual variability on the ensemble means and to estimate that variability as a function of altitude. For each case, the model was run for a year before the start of the study interval, to assure that minor chemical constituents had equilibrated. Lower boundary conditions specifying time-dependent trace gas inputs were the same as the standard reference case employed in the Chemistry Climate Model Initiative (Eyring et al., 2013) (see Table 1). Free-running climate simulations were employed, except that an empirical stratospheric quasi-biennial oscillation and observed sea surface temperatures were imposed. Monthly mean results were archived for all fields, and annual means of temperatures (neutral, ion, and electron), neutral density, electron density, and geopotential height were derived. Zonal mean annual means were then calculated and 5 year zonal means obtained from the annual means. The temperature differences between the 1972–1976 runs and the 2001–2005 runs were calculated on pressure surfaces and are shown in Figure 1 as a function of latitude and log pressure. The approximate altitudes corresponding to the pressure surfaces are shown on the rightside axis.

Global mean annual means and 5 year averages of the global means were calculated from the zonal means using cosine (latitude) weighting. The global mean profiles and changes for temperature and mass density are plotted in Figure 2. In Figures 2a and 2b, the temperatures and density profiles are plotted with respect to the global mean geometric altitude z , derived from geopotential height using the relationship $z = h/(1 - h/r_E)$, to account for the variation of gravitational acceleration (where h is geopotential height and r_E is the mean radius of the Earth) (Akmaev et al., 2010). The density change shown in Figure 2d

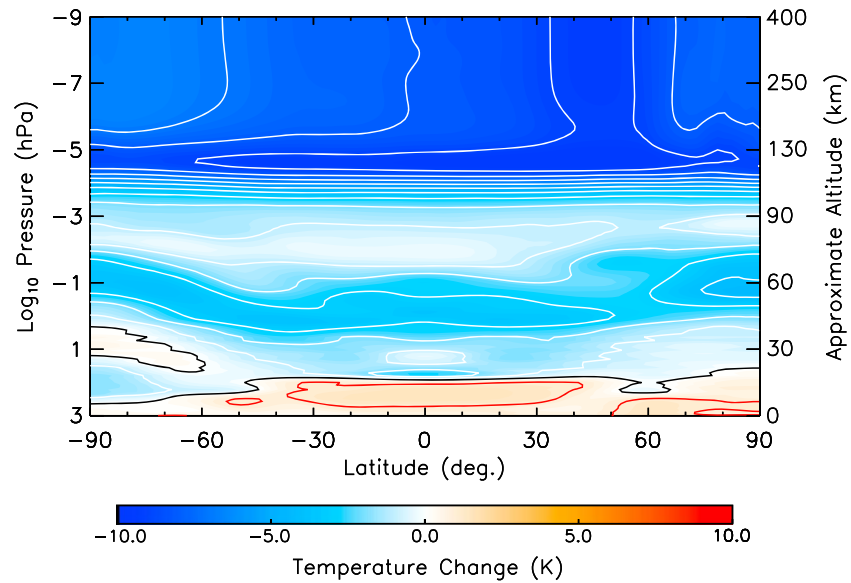


Figure 1. Model calculations of the zonal mean annual mean changes in temperature under low solar activity conditions, as a function of latitude and pressure, for the 29 year simulation period between 5 year ensembles (1972–1976 to 2001–2005). Negative contours, ranging from -9 to -1 K, with a 1 K interval, are shown in white; positive contours, at $+1$ and $+2$ K, are shown in red. The zero change line is shown in black.

is also plotted with respect to geometric altitude, with the 2001–2005 results interpolated onto the 1972–1976 altitudes. However, the temperature changes in Figure 2c are computed on pressure surfaces, similar to Figure 1, to avoid the misleading convolution of pressure level subsidence with cooling temperatures. The changes at key altitudes are summarized in Table 1, converted from the 29 year period between ensembles into K/decade, in order to facilitate comparison with other modeling and observational work.

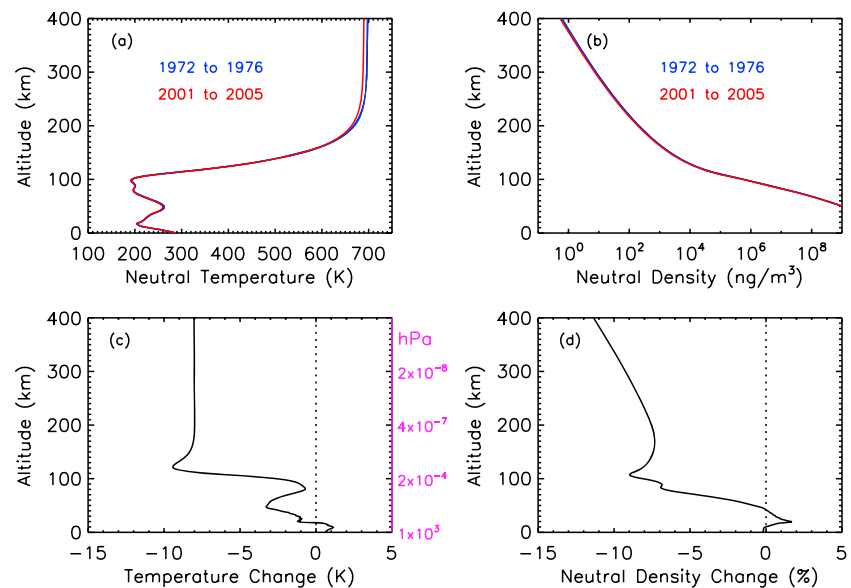


Figure 2. Model calculations of the modeled global mean annual mean changes, under low solar activity conditions, over the 29 year period between 5 year ensembles (1972–1976 to 2001–2005), with CO_2 levels at the surface increasing from 330 to 373 ppmv. (a) Temperature profiles as a function of altitude. Blue: 1972–1976 (T_1). Red: 2001–2005 (T_2). (b) Neutral mass density as a function of altitude. Blue: 1972–1976 (n_1). Red: 2001–2005 (n_2). (c) Temperature change as a function of pressure, $T_2 - T_1$. (d) Neutral number density percent change as a function of altitude, $100(n_2/n_1 - 1)$.

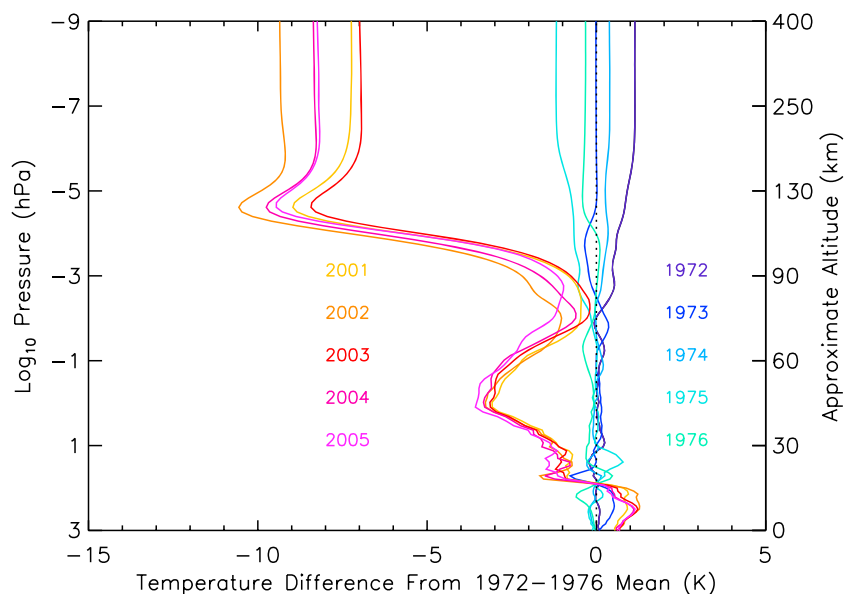


Figure 3. Interannual variability of global mean annual mean temperatures under constant low solar and geomagnetic activity conditions. Temperature difference from mean of 1972 to 1976 simulations, as labeled.

Interannual variations of global mean temperatures are explored in Figure 3. This is a plot of the difference between the global mean annual mean temperature in each year and the 1972–1976 mean. Although 10 years are not enough to fully quantify interannual variations, they yield a coherent result: the model variance in this very broad parameter is modest throughout the lower and middle atmosphere, a fraction of a degree Kelvin at most but increases to ~ 1 K near the mesopause. In the thermosphere, the variance remains on the order of 1 K but becomes smaller on a percentage basis as the temperature increases and of course is much smaller than the change induced by external solar/geomagnetic forcing, which is not included in these experiments.

4. Comparison to Previous Models and Observations

4.1. Troposphere

Since the sea surface temperatures used in these model runs were specified from measurements, model results for the lower troposphere are strongly influenced by this boundary condition, and no significant departure from the observed global temperature variation is expected. The modeled global average temperature change from 1972–1976 to 2001–2005 increases with altitude from $\sim +0.2$ K/decade at the surface to $\sim +0.4$ K/decade at ~ 10 km (266 hPa). Corresponding surface changes are $\sim +0.15$ K in the NCAR sea surface temperature analysis (Huang et al., 2015; Huang & National Center for Atmospheric Research Staff, 2017) and $\sim +0.2$ K/decade in the Goddard Institute for Space Studies land-sea temperature record (Hansen et al., 2010). This is in accord with various climate models as summarized by Intergovernmental Panel on Climate Change reports, which yield a model consensus $\sim +0.2$ K/decade increase in surface temperature (Intergovernmental Panel on Climate Change, 2014). The CESM v. 1.0 (CAM5) large ensemble run (Kay et al., 2015) also obtained an average of $\sim +0.2$ K/decade surface temperature increase during the years 1970–2000, as did Marsh et al. (2013), using WACCM4 and a fully coupled ocean. Garcia et al. (2007), using WACCM3, found $\sim +0.15$ K/decade at the surface, increasing to $\sim +0.3$ K/decade near 10 km altitude. Since WACCM-X is based on CAM and WACCM, it is unsurprising but reassuring that these results are in general agreement with those from other versions of the CESM.

4.2. Stratosphere

Results shown in Figures 1 and 2 exhibit a transition from tropospheric warming to -1.1 K/decade cooling at the stratopause, with the zero-crossing line just above the tropopause on a global average basis. This is similar to Garcia et al. (2007), who also found the zero crossing near the tropopause and -1.4 K/decade at the stratopause. Fomichev et al. (2007), using the Canadian Middle Atmosphere Model, estimated -10 K

temperature change at the stratopause for a doubled- CO_2 scenario, which translates to ~ -1.4 K/decade, assuming that temperature change is approximately linear with CO_2 increase. Marsh et al. (2013), comparing 2005 to a preindustrial case, found -8 K at the stratopause, which is also ~ -1.4 K/decade, under the same assumption. There is considerable structure in the zonal means, however, especially in the high-latitude southern hemisphere, with cooling in the lower stratosphere, likely due to O_3 reduction, but modulated by increasing vortex strength (Calvo et al., 2017). There is a very small temperature increase in the Southern Hemisphere middle stratosphere seen in Figure 1, and in Figure 5 of Garcia et al. (2007), but we agree with Garcia et al. (2007) that this is not statistically significant. Randel et al. (2017) compared global average temperature trends for 1979–1997, the period of maximum rate of O_3 depletion, to WACCM4, and found good agreement, with ~ -1 K/decade in the middle stratosphere and agreement with measured O_3 variability and trends.

4.3. Mesosphere

The model simulations show global mean cooling throughout the mesosphere but decreasing with altitude from -1.1 K/decade at the stratopause to -0.2 K/decade at the mesopause. This is similar to previous WACCM results (Garcia et al., 2007), earlier simulations by Akmaev and Fomichev (2000), Canadian Middle Atmosphere Model simulations (Fomichev et al., 2007), and the Leibniz-Institute Middle Atmosphere model (Lübken et al., 2013). Observational evidence is reviewed by Laštovička (2017), including the results from Huang et al. (2014) showing cooling on the order of -1 K/decade in the middle mesosphere and also reducing to nearly undetectable near the mesopause. Other observations reviewed by Laštovička, including ground-based lidar, radar, and optical measurements, yield inconsistent results near the mesopause, supporting the contention that the effects of anthropogenic change on this region of the atmosphere are still uncertain, since it is dynamically complex and has significant interannual variation, as discussed below.

4.4. Thermosphere

The thermosphere is the region of the atmosphere subject to the largest anthropogenic changes in temperature, on an absolute basis and also on a percentage basis. These cause even larger changes in density (at constant altitude), which is the primary means of detecting and quantifying the temperature change. However, the picture is complicated by variable solar ultraviolet and geomagnetic heating, both of which are manifestations of solar activity, especially on 11 year solar cycle time scales. Nevertheless, this is where upper atmosphere global change was first detected, by Keating et al. (2000), using the simple expedient of comparing three successive solar minimum periods. Independent analyses by Emmert et al. (2004, 2008, 2015), Marcos et al. (2005), and Saunders et al. (2011) have confirmed these findings, using various methods of accounting for solar activity but with considerable spread with regard to the magnitude of the rate of cooling. There has also been variation in the model estimates over the years, starting with the original 1-D calculation by Roble and Dickinson (1989) and continuing with 3-D global modeling, most recently using Thermosphere-Ionosphere-Mesosphere-Electrodynamics General Circulation Model (TIME-GCM) simulations (Qian et al., 2011, 2014; Solomon et al., 2015). For the low solar activity case, the measurements and models appear to be on a convergent path, but the dependence of the rate of change on the level of solar activity remains in doubt (Emmert, 2015) as discussed below. At any rate, there is unanimity with regard to the sign of the change and the reality of thermospheric cooling and contraction. This is summarized in Table 1, using density change at the benchmark 400 km altitude as the metric. There are other means of inferring neutral temperature change, including radar measurements of ion temperature T_i , which is strongly linked to neutral temperature up to the peak of the F region ionosphere ($h_m F_2$). Modeled change in T_i at $h_m F_2$ is shown in Table 1, as well as change in $h_m F_2$ and the peak density ($N_m F_2$). However, there was little or no change in the peak density of the E region ionosphere ($N_m E$) near 110 km. Ionospheric changes are not the focus of this letter but are reported here for comparison with the various measurement analyses. In the case of T_i work by Zhang et al. (2011, 2016), Zhang and Holt (2013) found -10 K/decade to -30 K/decade at various locations and altitudes. These results are much larger than observational estimates based on satellite drag (cf. Akmaev, 2012).

5. Discussion

The two 5 year simulations conducted for this study are equivalent to two ensembles of five 1 year runs. Each of them span just over two full cycles of the quasi-biennial oscillation, and both periods happen to contain

both phases of the Pacific Ocean Southern Oscillation. Five year ensembles would not be sufficient for fully characterizing regional troposphere-ocean climate variability but are sufficient for the purpose here of quantifying global mean upper atmosphere change and estimating its interannual variation. The intervals chosen also span the most significant period of stratospheric O₃ depletion through the 1970s and 1980s, reaching a broad minimum in the late 1990s. This is important in driving stratosphere and also mesosphere change but makes a very minor contribution to thermosphere/ionosphere change. CH₄ increase, which results in changes in middle-atmosphere water vapor and odd hydrogen, also has little effect on the thermosphere. CO₂ remains the primary driver of anthropogenic global climate change, throughout the atmosphere, but especially in the thermosphere, as shown by Qian et al. (2013).

Observational work has yielded inconsistent results in the mesopause region, and previous modeling work has predicted little or no global mean temperature trends. This is likely due to the dominance of dynamical processes in controlling mesopause temperature, which exhibit significant interannual variability, even without variable solar forcing. The seasonal-latitudinal behavior of trends could be important, however, especially with regard to the development of polar mesospheric clouds during the summer months, but on a global mean annual mean basis, any trends developing within the past several decades would still be within the envelope of interannual variance, as seen in Figure 3. Similarly, these simulations did not identify significant change in the lower ionosphere *E* region, although small observed trends have been reported (e.g., Bremer, 2008). Other controversial aspects of mesopause processes and trends relate to questions concerning changes in gravity waves, eddy diffusion, turbopause height, and their effects on CO₂ and atomic oxygen profiles. Recent work by Qian et al. (2017) and the analysis by Laštovička (2017) have laid to rest various speculative mechanisms in favor of the known ones: infrared cooling by molecules that are radiationally active in the infrared.

Model estimates of these radiative processes nevertheless contain considerable uncertainties, especially with regard to the collisional excitation/deactivation rates of CO₂ and nitric oxide (NO) with atomic oxygen (cf. Solomon et al., 2015). Similarly, quantifying the solar cycle effects on thermospheric density, both to remove it from trend analyses and to understand how these trends vary with the level of solar activity, remains a challenging problem. Although Emmert et al. (2008) found that thermospheric cooling is largest under solar minimum conditions and decreases with increasing solar activity, Emmert (2015) casts doubt on the statistical significance of this finding, because it now seems possible that solar ultraviolet irradiance and solar geomagnetic activity have been systematically decreasing over the past several cycles. This is especially a problem for solar minimum conditions, as explored by Solomon et al. (2010, 2011, 2013), which could be an issue for the original Keating et al. (2000) approach of comparing successive solar minima.

Another problem with observational evidence of thermospheric cooling is that analyses of T_i measured by ground-based radars appear to show cooling rates as much as an order of magnitude larger than those derived from satellite drag. These may also be affected by secular decline in solar activity, but interpretation of local ground-based sampling of the ionosphere can be problematical, due to secular variation of the magnetic field (e.g., Cnossen & Richmond, 2012). Regardless, a rate of change as large as -30 K/decade would cause a 50% reduction of thermospheric density over the 50 year span of radar and satellite drag data records, which would be conspicuous in other thermosphere and ionosphere measurements, including h_mF_2 .

6. Conclusion

Simulations of anthropogenic change show global mean annual mean temperatures increasing in the troposphere but decreasing in the upper atmosphere, from the lower stratosphere to the exobase, with the possible exception of the mesopause region. Although this observational and theoretical fact is sometimes considered paradoxical, it is instead a demonstration of the ability of numerical models to describe the complex dynamics, chemistry, and radiative transfer that occur throughout the atmosphere. There is general agreement between observations and models of the rate of temperature change as a function of altitude, but unresolved discrepancies do remain, particularly at altitudes that are difficult to measure accurately over extended time periods, such as the mesosphere and lower thermosphere. Since there are still some criticisms concerning the observational data and modeling techniques used to characterize temperature changes near the Earth's surface, there is risk that work by the international upper-atmosphere trends community may be deliberately misconstrued as confusion concerning the mechanisms of global change. Nevertheless, whole

atmosphere modeling demonstrates not only the complexity of atmospheric processes but also the success of comprehensive numerical simulations in describing them.

These simulations were conducted using perpetual solar minimum conditions, in order to eliminate the confounding effects of solar activity variation, especially in the thermosphere. Our next simulations will be for solar maximum, in order to investigate the solar cycle effect on the rate of change throughout the atmosphere. Subsequently, we will do a fully transient run, with all time-dependent lower boundary and solar/geomagnetic forcings and analyze the results using the same multivariate methods used to investigate observational data sets. We will also perform simulations with a fully coupled ocean model. These studies will better characterize the solar cycle and other dependencies, but the basic atmospheric response to anthropogenic change is revealed through the solar minimum case described here. These findings largely confirm earlier results using models describing limited atmospheric regions, but by performing simulations using a single integrated model, we demonstrate the ability of a consistent and comprehensive set of dynamics, physics, and chemistry to describe global change throughout the atmosphere.

Acknowledgments

The authors acknowledge the pioneering work by the progenitors of whole atmosphere modeling, Byron Boville, Rolando Garcia, and Ray Roble, and essential contributions by the many members of the WACCM, CAM, and CESM development teams. As a component of the Community Earth System Model, WACCM-X source code and results are publicly available at the NCAR web site. Model output data used in this letter are archived on the NCAR High Performance Storage System. This work was supported by NSF grant 1135432 and by NASA grants NNX14AH54G, NNX15AJ24G, and NNX16AB82G. NCAR is supported by the National Science Foundation.

References

- Akmaev, R. A. (2012). On estimation and attribution of long-term temperature trends in the thermosphere. *Journal of Geophysical Research*, 117, A09321. <https://doi.org/10.1029/2012JA018058>
- Akmaev, R. A., & Fomichev, V. I. (2000). A model estimate of cooling in the mesosphere and lower thermosphere due to the CO₂ increase over the last 3–4 decades. *Geophysical Research Letters*, 27, 2113–2116. <https://doi.org/10.1029/1999GL011333>
- Akmaev, R. A., Fomichev, V. I., & Zhu, X. (2006). Impact of middle-atmospheric composition changes on greenhouse cooling in the upper atmosphere. *Journal of Atmospheric and Solar - Terrestrial Physics*, 68(17), 1879–1889. <https://doi.org/10.1016/j.jastp.2006.03.008>
- Akmaev, R. A., Wu, F., Fuller-Rowell, T. J., Wang, H., & Iredell, M. D. (2010). Midnight density and temperature maxima, and thermospheric dynamics in Whole Atmosphere Model simulations. *Journal of Geophysical Research*, 115, A08326. <https://doi.org/10.1029/2010JA015651>
- Beig, G., Keckhut, P., Lowe, R. P., Roble, R. G., Mlynarczyk, M. G., Scheer, J., ... Fadnavis, S. (2003). Review of mesospheric temperature trends. *Reviews of Geophysics*, 41(4), 1015. <https://doi.org/10.1029/2002RG000121>
- Brasseur, G., & Hitchman, M. H. (1988). Stratospheric response to trace gas perturbations—Changes in ozone and temperature distributions. *Science*, 240(4852), 634–637. <https://doi.org/10.1126/science.240.4852.634>
- Bremer, J. (2008). Long-term trends in the ionospheric E and F₁ regions. *Annales Geophysicae*, 26(5), 1189–1197. <https://doi.org/10.5194/angeo-26-1189-2008>
- Calvo, N., Garcia, R. R., & Kinnison, D. E. (2017). Revisiting Southern Hemisphere polar stratospheric temperature trends in WACCM: The role of dynamical forcing. *Geophysical Research Letters*, 44, 3402–3410. <https://doi.org/10.1002/2017GL072792>
- Cnossen, I., & Richmond, A. D. (2012). How changes in the tilt angle of the geomagnetic dipole affect the coupled magnetosphere-ionosphere-thermosphere system. *Journal of Geophysical Research*, 117, A10317. <https://doi.org/10.1029/2012JA018056>
- Dickinson, R. E. (1984). Infrared radiative cooling in the mesosphere and lower thermosphere. *Journal of Atmospheric and Terrestrial Physics*, 46(11), 995–1008. [https://doi.org/10.1016/0021-9169\(84\)90006-0](https://doi.org/10.1016/0021-9169(84)90006-0)
- Emmert, J. T. (2015). Altitude and solar activity dependence of 1967–2005 thermospheric density trends derived from orbital drag. *Journal of Geophysical Research: Space Physics*, 120, 2940–2950. <https://doi.org/10.1029/2015JA021047>
- Emmert, J. T., Picone, J. M., Lean, J. L., & Knowles, S. H. (2004). Global change in the thermosphere: Compelling evidence of a secular decrease in density. *Journal of Geophysical Research*, 109, A02301. <https://doi.org/10.1029/2003JA010176>
- Emmert, J. T., Picone, J. M., & Meier, R. R. (2008). Thermospheric global average density trends 1967–2007, derived from orbits of 5000 near-Earth objects. *Geophysical Research Letters*, 35, L05101. <https://doi.org/10.1029/2007GL032809>
- Eyring, V., Lamarque, J.-F., Hess, P., Arfeuille, F., Bowman, K., Chipperfield, M. P., ... Young, P. (2013). Overview of IGAC/SPARC Chemistry-Climate Model Initiative (CCMI) community simulations in support of upcoming ozone and climate assessments. *SPARC Newsletter*, 40, 48–66.
- Fels, S. B., Mahlman, J. D., Schwarzkopf, M. D., & Sinclair, R. W. (1980). Stratospheric sensitivity to perturbations in ozone and carbon dioxide: Radiative and dynamical response. *Journal of the Atmospheric Sciences*, 37, 2265–2297. [https://doi.org/10.1175/1520-0469\(1980\)037%3C2265:SSTPIO%3E2.0.CO;2](https://doi.org/10.1175/1520-0469(1980)037%3C2265:SSTPIO%3E2.0.CO;2)
- Fomichev, V. I., Blanchet, J.-P., & Turner, D. S. (1998). Matrix parameterization of the 15 μ m CO₂ band cooling in the middle and upper atmosphere for variable CO₂ concentration. *Journal of Geophysical Research*, 103, 11,505–11,528. <https://doi.org/10.1029/98JD00799>
- Fomichev, V. I., Jonsson, A. I., de Grandpre, J., Beagly, S. R., McLandress, C., Semeniuk, K., & Shepherd, T. (2007). Response of the middle atmosphere to CO₂ doubling: Results from the Canadian middle atmosphere model. *Journal of Climate*, 20(7), 1121–1144. <https://doi.org/10.1175/JCLI4030.1>
- Garcia, R. R., Marsh, D. R., Kinnison, D. E., Boville, B. A., & Sassi, F. (2007). Simulation of secular trends in the middle atmosphere, 1950–2003. *Journal of Geophysical Research*, 112, D09301. <https://doi.org/10.1029/2006JD007485>
- Hansen, J., Ruedy, R., Sato, M., & Lo, K. (2010). Global surface temperature change. *Reviews of Geophysics*, 48, RG4004. <https://doi.org/10.1029/2010RG000345>
- Huang, B., Banzon, V. F., Freeman, E., Lawrimore, J., Liu, W., Peterson, T. C., ... Zhang, H. M. (2015). Extended reconstructed sea surface temperature version 4 (ERSST.v4). Part I: Upgrades and intercomparisons. *Journal of Climate*, 28(3), 911–930. <https://doi.org/10.1175/JCLI-D-14-00006.1>
- Huang, B., & National Center for Atmospheric Research Staff (Eds.) (2017). The climate data guide: SST data: NOAA extended reconstruction SSTs, version 4. Retrieved from <https://climatedataguide.ucar.edu/climate-data/sst-data-noaa-extended-reconstruction-ssts-version-4>
- Huang, F. T., Mayr, H. G., Russell, J. M. III, & Mlynarczyk, M. G. (2014). Ozone and temperature decadal trends in the stratosphere, mesosphere and lower thermosphere, based on measurements from SABER on TIMED. *Annales Geophysicae*, 32(8), 935–949. <https://doi.org/10.5194/angeo-32-935-2014>

- Hurrell, J. W., Holland, M. M., Gent, P. R., Ghan, S., Kay, J. E., Kushner, P. J., ... Marshall, S. (2013). The Community Earth System Model: A framework for collaborative research. *Bulletin of the American Meteorological Society*, 94(9), 1339–1360. <https://doi.org/10.1175/BAMS-D-12-00121.1>
- Intergovernmental Panel on Climate Change (2014). In Core writing team, R. K. Pachauri, & L. A. Meyer (Eds.), *Climate change 2014: Synthesis report. Contribution of working groups I, II and III to the fifth assessment report of the intergovernmental panel on climate change* (p. 151). Geneva, Switzerland: IPCC.
- Kay, J. E., Deser, C., Phillips, A., Mai, A., Hannay, C., Strand, G., ... Vertenstein, M. (2015). A community resource for studying climate change in the presence of internal climate variability. *Bulletin of the American Meteorological Society*, 96(8), 1333–1349. <https://doi.org/10.1175/BAMS-D-13-00255.1>
- Keating, G. M., Tolson, R. H., & Bradford, M. S. (2000). Evidence of long-term global decline in the Earth's thermospheric densities apparently related to anthropogenic effects. *Geophysical Research Letters*, 27, 1523–1526. <https://doi.org/10.1029/2000GL003771>
- Labitzke, K., Brasseur, G., Naujokat, B., & De Rudder, A. (1986). Long-term temperature trends in the stratosphere: Possible influence of anthropogenic gases. *Geophysical Research Letters*, 13, 52–55. <https://doi.org/10.1029/GL013i001p00052>
- Laštovička, J. (2017). A review of recent progress in trends in the upper atmosphere. *Journal of Atmospheric and Solar - Terrestrial Physics*, 163, 2–13. <https://doi.org/10.1016/j.jastp.2017.03.009>
- Laštovička, J., Akmaev, R. A., Beig, G., Bremer, J., & Emmert, J. T. (2006). Global change in the upper atmosphere. *Science*, 314(5803), 1253–1254. <https://doi.org/10.1126/science.1135134>
- Laštovička, J., Solomon, S. C., & Qian, L. (2012). Trends in the neutral and ionized upper atmosphere. *Space Science Reviews*, 168(1–4), 113–145. <https://doi.org/10.1007/s11214-011-9799-3>
- Lindzen, R. S. (1981). Turbulence and stress owing to gravity wave and tidal breakdown. *Journal of Geophysical Research*, 86, 9707–9714. <https://doi.org/10.1029/JC086iC10p09707>
- Liu, H.-L., Foster, B. T., Hagan, M. E., McInerney, J. M., Maute, A., Qian, L., ... Oberheide, J. (2010). Thermosphere extension of the Whole Atmosphere Community Climate Model. *Journal of Geophysical Research*, 115, A12302. <https://doi.org/10.1029/2010JA015586>
- Liu, H.-L., Bardeen, C. G., Foster, B. T., Lauritzen, P., Liu, J., Lu, G., ... Wang, W. (2018). Development and validation of the whole atmosphere community climate model with thermosphere and ionosphere extension (WACCM-X v. 2.0). *Journal of Advances in Modeling Earth Systems*, 10. <https://doi.org/10.1002/2017MS001232>
- Lübken, F.-J., Berger, U., & Baumgarten, G. (2013). Temperature trends in the midlatitude summer mesosphere. *Journal of Geophysical Research: Atmospheres*, 118, 13,347–13,360. <https://doi.org/10.1002/2013JD020576>
- Marcos, F. A., Wise, J. O., Kendra, M. J., Grossbard, N. J., & Bowman, B. R. (2005). Detection of a long-term decrease in thermospheric neutral density. *Geophysical Research Letters*, 32, L04103. <https://doi.org/10.1029/2004GL021269>
- Marsh, D. R., Garcia, R. R., Kinnison, D. E., Boville, B. A., Sassi, F., Solomon, S. C., & Matthes, K. (2007). Modeling the whole atmosphere response to solar cycle changes in radiative and geomagnetic forcing. *Journal of Geophysical Research*, 112, D23306. <https://doi.org/10.1029/2006JD008306>
- Marsh, D. R., Mills, M. J., Kinnison, D. E., Lamarque, J.-F., Calvo, N., & Polvani, L. M. (2013). Climate change from 1850 to 2005 simulated in CESM1 (WACCM). *Journal of Climate*, 26(19), 7372–7391. <https://doi.org/10.1175/JCLI-D-12-00558.1>
- Neale, R., Richter, J., Park, S., Lauritzen, P., Vavrus, S., Rasch, P., & Zhang, M. (2013). The mean climate of the Community Atmosphere Model (CAM4) in forced SST and fully coupled experiments. *Journal of Climate*, 26(14), 5150–5168. <https://doi.org/10.1175/JCLI-D-12-00236.1>
- Qian, L., Burns, A. G., Solomon, S. C., & Wang, W. (2017). Carbon dioxide trends in the mesosphere and lower thermosphere. *Journal of Geophysical Research: Space Physics*, 122, 4474–4488. <https://doi.org/10.1002/2016JA023825>
- Qian, L., Laštovička, J., Roble, R. G., & Solomon, S. C. (2011). Progress in observations and simulations of global change in the upper atmosphere. *Journal of Geophysical Research*, 116, A00H03. <https://doi.org/10.1029/2010JA016317>
- Qian, L., Marsh, D., Merkel, A., Solomon, S. C., & Roble, R. G. (2013). Effect of trends of middle atmosphere gases on the mesosphere and thermosphere. *Journal of Geophysical Research: Space Physics*, 118, 3846–3855. <https://doi.org/10.1002/jgra.50354>
- Qian, L., Roble, R. G., Solomon, S. C., & Kane, T. J. (2006). Calculated and observed climate change in the thermosphere, and a prediction for solar cycle 24. *Geophysical Research Letters*, 33, L23705. <https://doi.org/10.1029/2006GL027185>
- Qian, L., Solomon, S. C., & Roble, R. G. (2014). Secular changes in the thermosphere and ionosphere between two quiet Sun periods. *Journal of Geophysical Research: Space Physics*, 119, 2255–2262. <https://doi.org/10.1002/2013JA019438>
- Randel, W. J., Polvani, L., Wu, F., Kinnison, D. E., Zou, C.-Z., & Mears, C. (2017). Troposphere-stratosphere temperature trends derived from satellite data compared with ensemble simulations from WACCM. *Journal of Geophysical Research: Atmospheres*, 122, 9651–9667. <https://doi.org/10.1002/2017JD027158>
- Richmond, A. D., Ridley, E. C., & Roble, R. G. (1992). A thermosphere/ionosphere general circulation model with coupled electrodynamics. *Geophysical Research Letters*, 19, 601–604. <https://doi.org/10.1029/92GL00401>
- Rishbeth, H., & Roble, R. G. (1992). Cooling of the upper atmosphere by enhanced greenhouse gases—Modelling of thermospheric and ionospheric effects. *Planetary and Space Science*, 40(7), 1011–1026. [https://doi.org/10.1016/0032-0633\(92\)90141-A](https://doi.org/10.1016/0032-0633(92)90141-A)
- Roble, R. G., & Dickinson, R. E. (1989). How will changes in carbon dioxide and methane modify the mean structure of the mesosphere and thermosphere? *Geophysical Research Letters*, 16, 1144–1141.
- Roble, R. G., & Ridley, E. C. (1994). A thermosphere-ionosphere-mesosphere-electrodynamics general circulation model (TIME-GCM): Equinox solar cycle minimum simulations (30–500 km). *Geophysical Research Letters*, 21, 417–420. <https://doi.org/10.1029/93GL03391>
- Roble, R. G., Ridley, E. C., Richmond, A. D., & Dickinson, R. E. (1988). A coupled thermosphere/ionosphere general circulation model. *Geophysical Research Letters*, 15(12), 1325–1328. <https://doi.org/10.1029/GL015i012p01325>
- Saunders, A., Lewis, H., & Swinerd, G. (2011). Further evidence of long-term thermospheric density change using a new method of satellite ballistic coefficient estimation. *Journal of Geophysical Research*, 116, A00H10. <https://doi.org/10.1029/2010JA016358>
- Solomon, S. C., & Qian, L. (2005). Solar extreme-ultraviolet irradiance for general circulation models. *Journal of Geophysical Research*, 110, A10306. <https://doi.org/10.1029/2005JA011160>
- Solomon, S. C., Qian, L., & Burns, A. G. (2013). The anomalous ionosphere between solar cycles 23 and 24. *Journal of Geophysical Research: Space Physics*, 118, 6524–6535. <https://doi.org/10.1002/jgra.50561>
- Solomon, S. C., Qian, L., Didkovsky, L. V., Viereck, R. A., & Woods, T. N. (2011). Causes of low thermospheric density during the 2007–2009 solar minimum. *Journal of Geophysical Research*, 116, A00H07. <https://doi.org/10.1029/2011JA016508>
- Solomon, S. C., Qian, L., & Roble, R. G. (2015). New 3D simulations of climate change in the thermosphere. *Journal of Geophysical Research: Space Physics*, 120, 2183–2193. <https://doi.org/10.1002/2014JA020886>
- Solomon, S. C., Woods, T. N., Didkovsky, L. V., Emmert, J. T., & Qian, L. (2010). Anomalous low solar extreme-ultraviolet irradiance and thermospheric density during solar minimum. *Geophysical Research Letters*, 37, L16103. <https://doi.org/10.1029/2010GL044468>

- Zhang, S.-R., & Holt, J. M. (2013). Long-term ionospheric cooling: Dependency on local time, season, solar activity, and geomagnetic activity. *Journal of Geophysical Research: Space Physics*, 118, 3719–3730. <https://doi.org/10.1002/jgra.50306>
- Zhang, S.-R., Holt, J. M., Erickson, P. J., Goncharenko, L. P., Nicolls, M. J., McCready, M., & Kelly, J. (2016). Ionospheric ion temperature climate and upper atmospheric long term cooling. *Journal of Geophysical Research, Space Physics*, 121, 8951–8968. <https://doi.org/10.1002/2016JA022971>
- Zhang, S.-R., Holt, J. M., & Kurdzo, J. (2011). Millstone Hill ISR observations of upper atmospheric long-term changes: Height dependency. *Journal of Geophysical Research*, 116, A00H05. <https://doi.org/10.1029/2010JA016414>